Original Article

Influence of electrodeposition parameter control on morphology, hardness, and wear behavior of nickel coatings on electrolytic copper

Verenice Andrade Costa [1]
Maria Aparecida Pinto [2]
Elaine Carballo Siqueira Corrêa [3]
Nayara Aparecida Neres da Silva [2]*
Taíse Mate Manhabosco [4]

Abstract

This study investigates the electrodeposition of nickel coatings using a nickel sulfate-based electrolyte, aiming at applications in the steel industry, particularly in the protection of molds employed in the continuous casting of steel. The microstructure and, consequently, the functional properties of the coatings are strongly influenced by the electrodeposition parameters. The objective of this work was to evaluate the effect of deposition conditions on the morphology and wear resistance of the coatings, through a comparative analysis of two distinct experimental setups. Structural characterization revealed that processing under extreme parameters (Condition 1) resulted in morphological heterogeneity, characterized by the formation of nodular aggregates distributed across both the periphery and the central regions of the coating surface. The hardness values for Conditions 1 and 2 were 405.8 ± 58.8 HV and 377.6 ± 42.2 HV, respectively. Similarly, the wear track volumes were (4.55 ± 0.63) × 10^{-3} mm^3 for Condition 1 and (4.90 ± 0.68) × 10^{-3} mm^3 for Condition 2. Both the hardness and wear volume data exhibit trends that fall within the margins of measurement uncertainty. Despite a nominal increase in mechanical performance, the overlapping uncertainty intervals suggest no statistically significant difference between the conditions. These findings underscore the necessity of precise electrodeposition parameter control to ensure coating reliability in industrial applications.

Keywords: Nickel coating; Electrodeposition; Process parameter control; Wear resistance.

1 Introduction

In the steel industry, nickel is an essential alloying element in the production of various steel grades and is also extensively employed as a coating material for continuous casting molds with copper substrates. This application is globally adopted due to the superior performance of nickel-coated plates, which exhibit extended operational lifetimes and can withstand numerous casting cycles before requiring recoating [1]. The thermal properties of nickel are relatively close to those of copper, a characteristic that likely contributes to the formation of deposits with lower internal stress accumulation. Reported values indicate that the thermal expansion coefficients of copper (20.3 × 10^{-6} K^{-1} from 20–1000 °C) and nickel (16.3 × 10^{-6} K^{-1} from 20–900 °C) are of comparable magnitudes. Furthermore, although the thermal conductivity of nickel at ~900 °C (71.6 $W \cdot m^{-1} \cdot K^{-1}$) is significantly lower than that of copper (244 $W \cdot m^{-1} \cdot K^{-1}$ at ~1000 °C), it remains sufficiently high to mitigate thermal gradients within the mold during operation [1,2].

According to the literature [1], nickel electrodeposition enables effective control over mechanical and structural properties such as hardness, ductility, and tensile strength, which are crucial for ensuring mold performance. Moreover, electrodeposition is characterized by operational simplicity, cost-effectiveness, and adaptability [3,4]. Developed in 1916, the Watts Nickel Process represents a milestone in the evolution of electrodeposition techniques and remains widely used in industrial practice due to its operational stability, formulation robustness, economic viability, and ease of commercial implementation [4,5].

[1]*Programa de Pós-Graduação em Engenharia de Materiais – REDEMAT, Escola de Minas, Universidade Federal de Ouro Preto – UFOP, Ouro Preto, MG, Brasil.*
[2]*Departamento de Engenharia Metalúrgica e de Materiais, Escola de Minas, Universidade Federal de Ouro Preto – UFOP, Ouro Preto, MG, Brasil.*
[3]*Departamento de Engenharia de Materiais, Centro Federal de Educação Tecnológica – CEFET-MG, Belo Horizonte, MG, Brasil.*
[4]*Departamento de Física, Instituto de Ciências Exatas e Biológicas, Universidade Federal de Ouro Preto – UFOP, Ouro Preto, MG, Brasil.*

**Corresponding author: nayara.neres@ufop.edu.br*
E-mails: andradecostav@gmail.com; mariap@ufop.edu.br; elainecarballo@cefetmg.br; taise@ufop.edu.br

The bath composition, consisting primarily of nickel sulfate, nickel chloride, boric acid, and organic additives, plays a central role in determining deposit uniformity, grain refinement, internal stress, and hardness. Surfactants are particularly effective in minimizing porosity and pitting, and saccharin can increase the cathodic overpotential, refine the grain structure, and contribute to internal stress reduction by promoting a shift from tensile to compressive stress states [6-11]. As noted by Di Bari [4], deposit characteristics depend not only on bath composition but also on the specific influence of each constituent on coating development. Chloride ions, for instance, increase the limiting current density and promote deposit uniformity. Boric acid mitigates hydrogen evolution and helps prevent cracking. Surfactants regulate surface tension, thereby reducing porosity and corrosion pit formation.

In addition to electrolyte composition, process parameters such as current density, temperature, and agitation critically affect coating morphology and performance. Moderate current densities and temperatures enhance mass transport and reduce hydrogen-related defects, although excessive current densities and temperatures may increase porosity and dendritic growth [4,6,12-14]. The resulting microstructure is governed by the adsorption of chemical species at the cathode surface and the suppression of hydrogen evolution and nickel hydroxide formation [4,15]. Previous studies [15] indicate that increasing current density leads to finer grain sizes but may also enhance porosity. Under optimized conditions, coatings produced from nickel sulfate baths with suitable additives typically exhibit hardness values ranging from 230 HV to 400 HV [15-17]. It is also important to mention the role of bath agitation, which aids in maintaining electrolyte homogeneity and facilitates gas bubble removal, while the use of demineralized and filtered water is essential to prevent contamination and undesired precipitation within the system [4,6].

Achieving uniform coatings with appropriate hardness and wear resistance remains a critical objective in nickel electrodeposition, particularly when balancing process feasibility and performance requirements. Therefore, this work aims to investigate the influence of electrodeposition parameters on the microstructural evolution, hardness, and tribological properties of nickel coatings.

The analysis focuses on the effects of current density, pH, and temperature on morphology, mechanical integrity and wear behavior of the electrodeposited layers.

2 Development

2.1 Materials and methods

The substrate used for the electrodeposition process consisted of electrolytic copper sheets. Prior to deposition, the substrates were mechanically cleaned with abrasive material and chemically etched in a 10% hydrochloric acid solution (to remove surface oxides and contaminants). Electrodeposition was performed using an Agilent U8032A power supply (0–60 V / 3 A and 5 V / 3 A). The experimental setup consisted of a magnetic stirring and heating plate equipped with a thermocouple (IonLab, model HJ-3 XMTE-205). A glass beaker was used, containing a copper cathode and a graphite anode; the latter served as an inert electrode to prevent further interference from anodic reactions during the deposition process.

The electrolyte solution was composed of nickel sulfate (270 g/L), nickel chloride (60 g/L), boric acid (37.5 g/L), saccharin (1.7 g/L), and sodium dodecyl sulfate (0.3 g/L). Coatings were produced under two different experimental conditions [6,11]:

- Condition 1: An intentionally extreme scenario for the applied temperature, pH and current density. During the process, the temperature increased from approximately 45 °C to 70 °C, the current density reached ~11.5 A/dm^2, and the bath pH decreased to about 1.7.

- Condition 2: All parameters were strictly controlled. The solution temperature was maintained at 45 ± 5 °C, the current density at approximately 4.5 A/dm^2, and the pH was adjusted to 3.8 by reducing the boric acid concentration compared to the first condition.

In both cases, electrodeposition was conducted for 10 min over an effective deposition area of approximately 520 mm^2. The electrodeposited samples were characterized in terms of surface morphology and cross-sectional structure. For cross-sectional analysis, the coatings were sectioned using an IsoMet 1000 precision cutter equipped with a diamond blade. To preserve coating integrity, the samples were oriented so that the blade rotation direction prevented delamination of the deposited layer. Subsequently, the specimens were cold mounted in acrylic resin and prepared through sequential grinding with 1200, 2400, and 4000 mesh abrasive papers, followed by polishing with diamond pastes of 3 μm and 1 μm particle sizes.

Morphological and microstructural examinations were carried out using scanning electron microscopy (SEM) with a Tescan Vega 3 system coupled to an Oxford X-Act (PentaFET Precision) energy-dispersive spectroscopy (EDS) detector. The wear behavior of the nickel coatings was evaluated using a ball-on-plate tribometer configuration (RTEC tribometer) under dry sliding conditions. The reciprocating wear test parameters were: 10 N applied load, sliding velocity of 3 mm/s, total wear track of 3 m, and a test duration of 1.5 h. The counterbody consisted of an alumina ball with a diameter of 6 mm. The wear profile and volume were obtained using a profilometer integrated with the tribometer system.

Additionally, ultramicrohardness tests were performed using a Dynamic Ultra Micro Hardness Tester (DUH-211S,

SHIMADZU) in load–unload mode. All tests were conducted under a constant load of 10 mN as described in previous studies [18,19]. Ten indentations were randomly distributed across each coating surface, in accordance with ASTM E384:2022 [20] and ISO 4516 [21] standards [22-24].

2.2 Results and discussion

Condition 1 was conducted outside the recommended process parameter range. Specifically, the temperature (45–70 °C) and applied current density (~11.5 A/dm^2) exceeded the values typically used in industry for nickel sulfate-based baths to produce uniform microstructures [4,6,12,13].

Figure 1a and 1b shows the coating edge and center, obtained under Condition 1. The formation of nodular features is clearly visible. The presence of nodules or dendritic structures in these regions suggests that the process parameters, particularly current density and temperature, surpassed the optimal range. These observations are consistent with previously reported studies [12,23,25]. Additionally, the coating appears to replicate the rough morphology of the substrate, which likely results from surface preparation prior to deposition.

High current densities during electrodeposition promote the nucleation of new grains both directly, by increasing the number of metal ions reduced per unit area and indirectly, by altering local conditions that affect deposit morphology. An increase in current density intensifies ionic depletion near the electrode surface, enhancing the local cathodic potential. This increase promotes ion migration toward the electrode, favoring nucleation and grain refinement in the resulting microstructure [26].

However, when the applied current density exceeds the diffusion-limited current (iL), significant changes occur in the deposition mechanism. Under such conditions, the transport of metal ions to the cathode becomes insufficient relative to the applied current, thereby promoting hydrogen evolution at the electrode–electrolyte interface. This phenomenon can lead to coatings with undesirable characteristics, such as high porosity, spongy texture, or a powdery appearance, all of which negatively impact coating quality and performance [15]. Nevertheless, although the current density applied in Condition 1 exceeded typical industrial values, SEM micrographs (Figure 1) did not reveal a significant presence of pores. This may be attributed to the electrolyte composition, specifically, the boric acid concentration and the action of the anionic surfactant sodium dodecyl sulfate, which may have minimized defect formation during deposition [6,15].

The formation of nodular and dendritic structures in electrodeposited coatings is closely linked to thermal and solute diffusion conditions, which govern the solid–liquid interface dynamics during growth. At higher temperatures, increased solubility of bath constituents enhances electrical conductivity and ionic diffusion, thereby promoting more efficient ion transport to the cathode and facilitating nucleation [15]. However, these beneficial effects are limited to a safe operational range (40–60 °C). Exceeding this range can result in degradation of organic additives within the bath, compromising their function, deteriorating coating mechanical properties, and contaminating the electrolyte. Additionally, excessive temperatures increase hydrogen adsorption at the cathode surface, leading to reduced deposit integrity. Another detrimental effect is exaggerated grain growth, which significantly decreases the mechanical strength of the electrodeposited layer [4,26].

Figures 1(c,d) show the SEM micrographs of the coating surface obtained under Condition 2, where all parameters were strictly controlled throughout electrodeposition. A high degree of deposit uniformity was observed under Condition 2 if compared to Condition 1, with the coating following the substrate topography and showing no nodular or dendritic formations. These results highlight the importance of precise control over process parameters such as temperature and current density, which in this condition were maintained within the limits recommended in the literature [7,15,22,23].

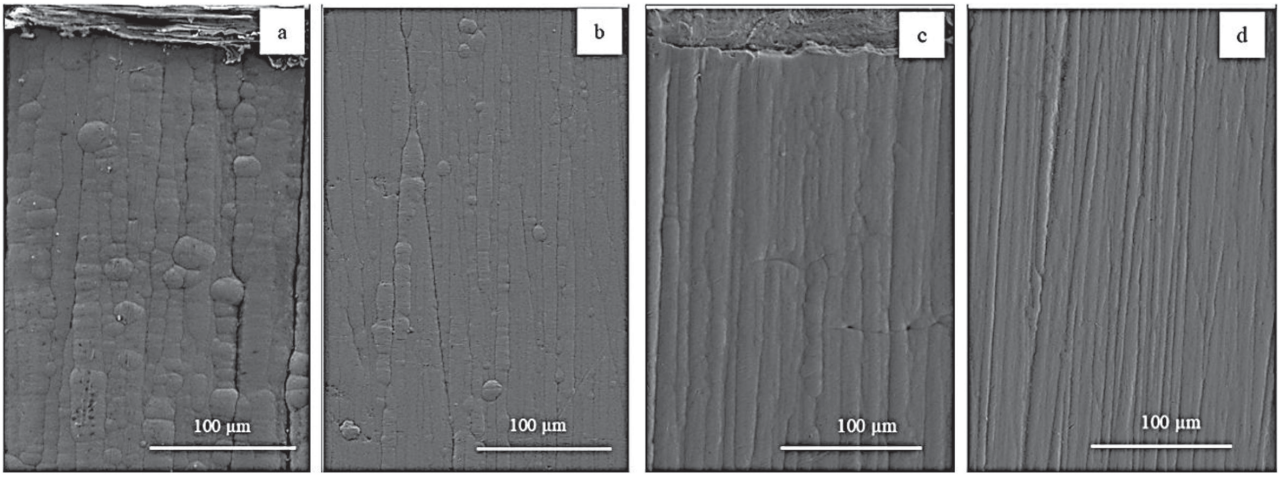

Figure 1. SEM images of the coating edge (a) and central region of the coating (b) for Condition 1, i. e., T ~ 70 ^{0}C, i ~ 11.5 A/dm^2, and pH ~1.7. SEM images of the coating edge (c) central region of the coating (d) for Condition 2, i. e., T ~ 45 ^{0}C, i ~ 4.5 A/dm^2 and pH ~3.8.

Figure 2 presents the SEM/EDS cross-sectional analyses of coatings produced under both experimental conditions. In both cases, the nickel distribution along the coating thickness is homogeneous, without discontinuities and suggesting negligible porosity. The average coating thicknesses were approximately 19 µm for Condition 1 (current density: 11.5 A/dm^2) and 5 µm for Condition 2 (current density: 4.5 A/dm^2), confirming the direct influence of temperature and current density on the deposition rate.

Under Condition 1, the higher current density and temperature accelerated metal ion reduction, producing thicker coatings for the same deposition time. Conversely, Condition 2, operated under optimized literature-based parameters, yielded thinner but more homogeneous coatings. It is important to emphasize, however, that higher thickness does not necessarily correlate with improved coating properties, which are influenced by a complex interplay of electrochemical and structural factors. Therefore, to achieve a coating with favorable microstructure and properties, it is crucial to establish a good balance between the operational parameters.

For the ultra-microhardness tests, the measured values were: 405.8 ± 58.8 HV for Condition 1 and 377.6 ± 42.2 HV for Condition 2. Although Condition 1 presented slightly higher nominal values, the associated error ranges indicate that this difference is not statistically significant. Condition 1 (i.e., higher current densities) promotes higher nucleation rates, which may result in grain refinement; however, the subject needs further investigation.

Figure 3 presents the results of the ball-on-plate wear tests performed under a normal load of 10 N, a sliding velocity of 3 mm/s, a wear track length of 3 mm, and a total duration of 1.5 h. The wear tracks exhibit mean width values of 280 35 µm and 300 µm 18 µm for Conditions 1 and 2, respectively. However, width and depth measurements may not fully represent the system's behavior, as Figure 3(a) clearly shows fluctuations along the track. Consequently, the volumetric loss (wear volume) stands as the most reliable

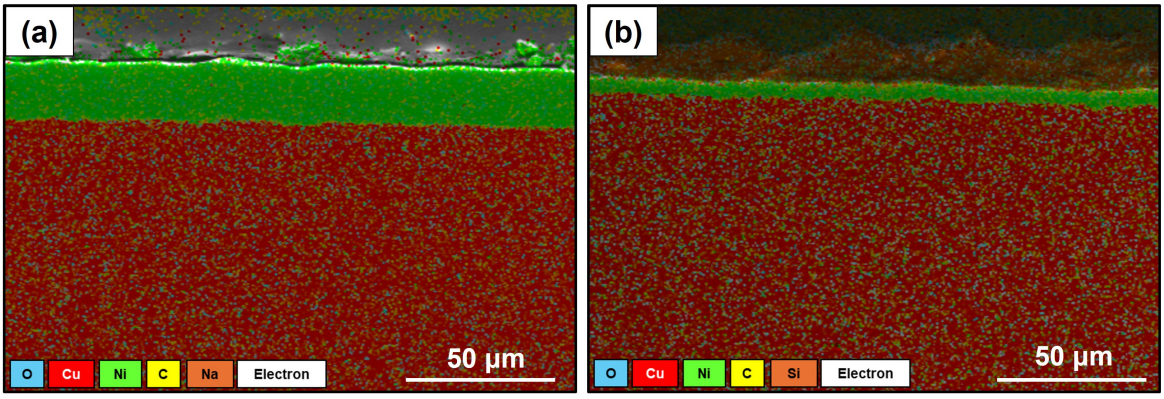

Figure 2. SEM/EDS micrographs showing the cross-sectional morphology and thickness of nickel coatings obtained under Condition 1(a) and Condition 2(b). Nickel coating (green) thickness: ~19 µm (a). Nickel coating (green) thickness: ~5 µm (b) [24].

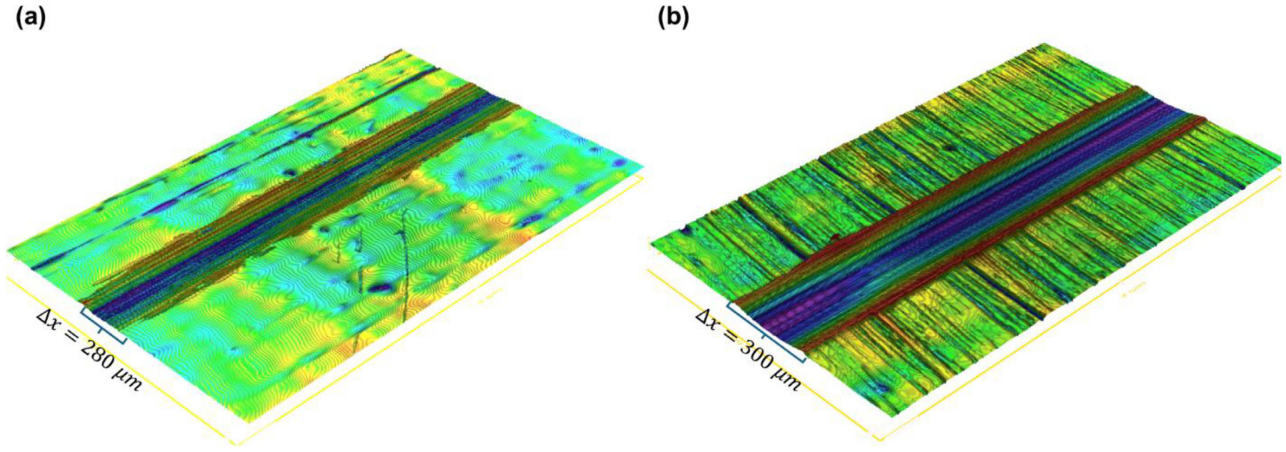

Figure 3. Representative wear tracks on nickel coatings obtained from ball-on-plate reciprocating tests under a normal load of 10 N and a sliding speed of 3 mm·s^{-1}: (a) coating produced under electrodeposition parameters outside the literature-recommended range (Condition 1) and (b) coating produced under electrodeposition parameters within the literature-recommended range (Condition 2).

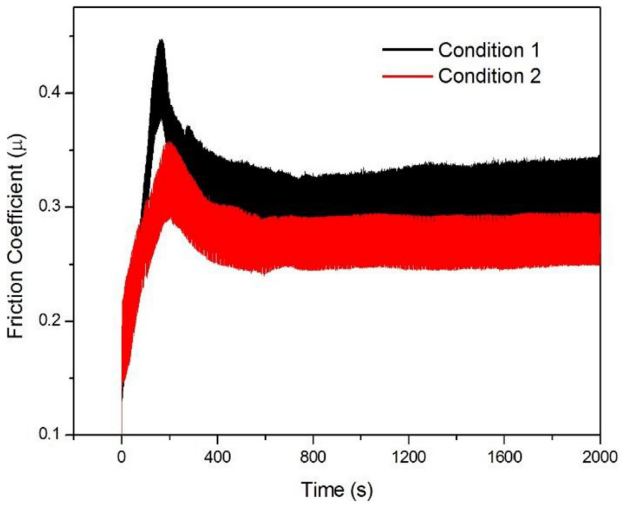

Figure 4. Evolution of friction coefficient from ball-on-plate test performed at 10 N, 3 mm/s, 5,400 s (2,000 s interval presented). Cond 1 and 2 are referred to coatings deposited at Condition 1 (70°C, i ~ 11.5 A/dm^2, and pH ~1.7e) and Condition 2 (T ~ 45 °C, i ~ 4.5 A/dm^2 and pH ~3.8).

parameter to quantify the wear damage. Wear track profiles obtained after testing were used to calculate wear volumes of $(4.55 \pm 0.63) \times 10^{-3}$ mm^3 and $(4.90 \pm 0.68) \times 10^{-3}$ mm^3 for Conditions 1 and 2, respectively. As observed in the hardness tests, the obtained values and their respective error ranges indicate that the difference lacks statistical significance.

For the coatings produced under both conditions, a run-in period was observed, corresponding to the initial sliding between bare surfaces. After this stage, the coefficient oscillated around average values of (0.280.05) and (0.310.04) for Conditions 1 and 2, respectively, as shown in the graph presented in Figure 4.

The run-in period is characterized by an initial increase in friction due to asperity wear and the subsequent generation of wear debris within the contact zone. This effect was more pronounced for Condition 1, which presented a rougher surface characterized by the presence of nodular features.

Overall, when analyzing the wear property values obtained for Conditions 1 and 2 while considering the variations associated with experimental error, no significant difference is observed between the two conditions. The occurrence of porosity and pitting, as reported in the literature [6,15] to result from high current density and low pH, is not likely to have produced a pronounced influence under Condition 1, since such effects could be detrimental to wear performance. However, these results do not imply that Condition 1 is superior for industrial applications. Coating uniformity, process reproducibility, and repeatability must also be considered.

3 Conclusion

The results demonstrate that strict control of electrodeposition parameters is crucial to obtain nickel coatings with uniform morphology and reliable performance. Although higher deposition rates were achieved under the condition with parameters outside the range applied in industry, the associated surface heterogeneity limits their suitability for industrial application. In contrast, operation within recommended parameter ranges produced more homogeneous coatings with stable mechanical and tribological behavior. These findings highlight that process control is a key requirement for the technological application of electrodeposited nickel coatings, particularly for components subjected to wear in industrial environments.

Acknowledgements

The authors gratefully acknowledge the financial support provided by FAPEMIG through the research projects APQ-03726-23 and APQ-03032-25.

References

1 Parkinson R. Nickel plating and electroforming: Essential industries for today and the future. Toronto: Nickel Development Institute; 2001.

2 Nix FC, MacNair D. The thermal expansion of pure metals: Copper, gold, aluminum, nickel, and iron. Physical Review. 1941;60(8):597-605.

3 Yue B, Zhu G, Chang Z, Song J, Gao X, Wang Y, et al. Study on surface wettability of nickel coating prepared by electrodeposition combined with chemical etching. Surface and Coatings Technology. 2022;444:128695.

4 Di Bari GA. Electrodeposition of nickel. Modern Electroplating. 2000;5:79-114.

5 Ak Azem NF, Birlik I. Influence of bath composition on the structure and properties of nickel coatings produced by electrodeposition technique. Deu Muhendis Fak Fen ve Muhendis. 2018;20(59):689-697.

6 Djouani R, Qian X. Mechanism of electrodeposition of nickel. International Journal of Current Research. 2018;10(01):64228-64239.

7 Rose I, Whittington C. Nickel plating handbook. Beijing: Nickel Institute; 2013. p. 263-292.

8 Mandich NV, Baudrand DW. Troubleshooting electroplating installations: Nickel sulfamate plating systems. Plating and Surface Finishing. 2002;89(9):68-76.

9 Yasin G, Anjum MJ, Malik MU, Khan MA, Khan WQ, Arif M, et al. Revealing the erosion-corrosion performance of sphere-shaped morphology of nickel matrix nanocomposite strengthened with reduced graphene oxide nanoplatelets. Diamond and Related Materials. 2020;104:107763.

10 Li YW, Huang XX, Yao JH, Deng XS. Effect of saccharin addition on the electrodeposition of nickel from a Watts-type electrolyte. Advanced Materials Research. 2011;189–193:911-914.

11 Rashidi AM, Amadeh A. The effect of saccharin addition and bath temperature on the grain size of nanocrystalline nickel coatings. Surface and Coatings Technology. 2009;204(3):353-358.

12 Poroch-Seriţan M, Bulai P, Severin TL, Gutt G. Modelling and optimization study on hardness of Ni-Fe alloy thin films through electroplating process. Applied Mechanics and Materials. 2014;657:286-290.

13 Kendrick RJ. High-Speed Nickel Plating from Sulphamate Solutions. Trans IMF. 1964;42(1):235-245.

14 Saleem M, Brook PA, Cuthbertson JW. Note on the structure of nickel deposited from sulphamate solutions. Electrochimica Acta. 1967;12(5):553-555.

15 Lins VFC, Cecconello ES, Matencio T. Effect of the current density on morphology, porosity, and tribological properties of electrodeposited nickel on copper. Journal of Materials Engineering and Performance. 2008;17(5):741-745.

16 Sanz A. Tribological behavior of coatings for continuous casting of steel. Surface and Coatings Technology. 2001;146–147:55-64.

17 Fattah M, Morin S. Microstructure, corrosion, and hardness properties of Ni coatings electrodeposited from a deep eutectic solvent-based electrolyte. Journal of Materials Engineering and Performance. 2024;34(17):18560-18576.

18 Dikici T, Culha O, Toparli M. Study of the mechanical and structural properties of Zn-Ni-Co ternary alloy electroplating. Journal of Coatings Technology and Research. 2010;7(6):787-792.

19 Chen JS, Duh JG, Wu FB. Microhardness and corrosion behavior in CrN / electroless Ni / mild steel complex coating. Surface and Coatings Technology. 2002;150(2-3):239-245.

20 American Society for Testing and Materials. ASTM E384-22: standard test method for microindentation hardness of materials. West Conshohocke: ASTM International; 2022.

21 International Organization for Standardization. ISO 4516: metallic and other inorganic coatings — Vickers and Knoop microhardness tests. Geneva: ISO; 2002.

22 Boukhouiete A, Boumendjel S, Sobhi NE. Effect of current density on the microstructure and morphology of the electrodeposited nickel coatings. Turkish Journal of Chemistry. 2021;45(5):1599-1608.

23 Cecconello ES. Morfologia e porosidade de níquel eletrodepositado em cobre [dissertação]. Belo Horizonte: Universidade Federal de Minas Gerais; 2006.

24 Costa VA, Silva NAN, Manhabosco TM. Influência do controle dos parâmetros de eletrodeposição na qualidade do revestimento de níquel sobre substrato de cobre eletrolítico. Tecnol em Metal Mater e Mineração. 2025;22:e3211.

25 Raghavendra CR, Basavarajappa S, Sogalad I, Kumar S. A review on Ni based nano composite coatings. Materials Today: Proceedings. 2020;39:6-16.

26 Wang W, Lee PD, McLean M. A model of solidification microstructures in nickel-based superalloys: Predicting primary dendrite spacing selection. Acta Materialia. 2003;51(10):2971-2987.

Received: 23 Oct. 2025
Accepted: 18 Feb. 2026

Editor-in-charge:
André Luiz Vasconcellos da Costa e Silva